The *Euplotes* La Motif Protein p43 Has Properties of a Telomerase-Specific Subunit†

Stefan Aigner,‡ Jan Postberg,§ Hans J. Lipps,§ and Thomas R. Cech*,‡

Department of Chemistry and Biochemistry and Howard Hughes Medical Institute, University of Colorado, Boulder, Colorado 80309-0215, and Institute of Cell Biology, University Witten/Herdecke, Stockumer Strasse 10, 58453 Witten, Germany

Received January 21, 2003; Revised Manuscript Received March 11, 2003

ABSTRACT: Telomerase is a specialized reverse transcriptase synthesizing DNA repeats at telomeres. In addition to the RNA and catalytic protein components, telomerase from the ciliate *Euplotes aediculatus* contains the subunit p43. This protein is homologous to the La autoantigen, functioning in maturation of RNA polymerase III transcripts. Here we provide evidence that p43 is primarily associated with the telomerase ribonucleoprotein in vivo. Recombinant p43 binds telomerase RNA with low-nanomolar affinity in vitro, recognizing stem I and adjacent nucleotides or structures in the core of the RNA. Unlike authentic La proteins, p43 does not bind strongly to RNA polymerase III precursor transcripts and does not exhibit a marked binding preference for 3′-terminal oligouridylate residues. In isolated macronuclei, p43 largely colocalizes with telomerase RNA in discrete foci. These findings suggest that p43 is not the *Euplotes* La protein but instead plays a dedicated role in telomerase assembly and/or function. Thus, p43 joins the telomerase reverse transcriptase and the yeast proteins Est1p and Est3p as the only telomerase-specific proteins identified so far.

A catalytic protein subunit (TERT)[1] and an intrinsic RNA component form the core of the RNP enzyme telomerase. Typically, however, telomerase complexes from different organisms contain additional protein factors. Some of these function in the maturation and stability of the telomerase RNP via binding to conserved RNA motifs near the 3′-end. For example, yeast telomerase RNA contains a functional Sm protein binding site common to spliceosomal RNAs (*1*). Vertebrate telomerase RNAs share a box H/ACA small nucleolar (sno) RNA domain (*2*, *3*), and the human RNA interacts with dyskerin (*4*), hGAR1 (*5*), and other box H/ACA-specific proteins (*6*). Other telomerase-associated proteins are molecular chaperones that bind TERT and promote assembly of the active RNP, such as human p23, hsp90 (*7*), and hsp70 (*8*) and probably their orthologs in *Tetrahymena* (*9*). The role of these proteins in telomerase has largely been deduced from their functions in other RNPs and protein complexes, where they have been extensively studied.

In contrast, we are just beginning to understand the functions of bona fide telomerase-specific proteins aside from TERT. Only two proteins of this type, yeast Est1p and Est3p (*10*, *11*), are known to date, and a function has so far only been described for Est1p. This protein recognizes a stem−bulge motif in the RNA (*12*) and facilitates recruitment of telomerase to the telomere (*13*) or, alternatively, activates telomere-bound telomerase (*14*). In this study, we provide evidence that p43 from the ciliate *Euplotes aediculatus* (*15*, *16*) is another telomerase-specific protein.

Telomerase is critical for chromosomal stability in most eukaryotes because it adds tandem repeats of a short GT-rich sequence to the telomeres, thereby counteracting chromosome shortening due to incomplete replication and nucleolytic degradation (for a review, see ref *17*). Catalysis of telomeric DNA synthesis by telomerase is templated by a portion of the RNA subunit (*18*); therefore, this enzyme is a reverse transcriptase. In addition to the functional conservation of telomerase across species, its structural conservation is evident by the presence of reverse transcriptase motifs (*19*) as well as telomerase-specific motifs (*20*) in all TERTs. In contrast, both the primary sequence of the RNA subunit and its size have diverged substantially during evolution. Moreover, telomerase RNAs are transcribed by RNA polymerase III (pol III) in ciliates but are pol II transcripts in yeast (*21*) and probably in vertebrates (*3*, *22*). Nevertheless, phylogenetic analysis has shown that vertebrate telomerase RNAs [size range of 382−559 nucloetides (nt)] can be modeled to assume a core secondary structure similar to that of their shorter (148−209 nt) ciliate homologues (*3*), for which such a model was first developed (*14*, *23*−*25*). Thus, the RNAs from these diverse species may be structurally related. It remains to be seen whether this is also true for the RNAs from budding yeast (*26*, *27*), which are typically ∼1 kb in length.

TERT was first identified in the ciliate *E. aediculatus* by a biochemical approach (*15*, *19*). The active purified complex was found to contain a single additional polypeptide (*15*), a 43 kDa protein termed p43. This protein is thought to be

† This work was supported by NIH Grant GM28039 (to T.R.C.) and a Deutsche Forschungsgemeinschaft grant (to H.J.L.).

* To whom correspondence should be addressed. Phone: (303) 492-8606. Fax: (303) 492-6194. E-mail: thomas.cech@colorado.edu.

‡ University of Colorado.

§ University Witten/Herdecke.

[1] Abbreviations: TERT, telomerase reverse transcriptase; RNP, ribonucleoprotein.

10.1021/bi034121y CCC: $25.00
Published on Web 04/23/2003

derived from its 51 kDa precursor by proteolysis and is associated with most or all active telomerase complexes (*16*).

By amino acid sequence analysis, p43 has a La motif relating it to the La autoantigen (*16*), an abundant primarily nuclear phosphoprotein found in a variety of eukaryotes (for a review, see ref *28*). It is well-established that La primarily recognizes the 3′-terminal oligouridylate sequence common to all pol III transcripts (*29*, *30*), but it has been difficult to ascribe a single function to this protein. Among other roles, La has been shown to be involved in the biogenesis of pol III transcripts by stabilizing these small RNAs from exonucleolytic degradation, contributing to their nuclear retention, and facilitating their correct processing. It is these roles of La that led to the proposal that La may act as a molecular chaperone for small RNAs (*31*, *32*). Ciliate telomerase RNAs are pol III transcripts (*18*, *24*, *33*, *34*), and retain their 3′-U's in the mature RNP (*18*, *24*), so it was not surprising to find a La homologue in the telomerase complex. However, the limited overall sequence homology between p43 and La (*16*) and the fact that La proteins are only associated with RNAs during their maturation, but are usually not found in mature RNPs, prompted us to study the in vivo association of p43 with other macromolecular complexes as well as its in vitro RNA binding specificity. We find that p43 is primarily associated with telomerase in the cell, not with other pol III transcripts. Furthermore, it shows a decided preference for the ciliate telomerase RNA structure. These results suggest that p43 may be the first bona fide telomerase-specific protein found in a species outside the yeasts.

MATERIALS AND METHODS

Gel Filtration Analysis of Nuclear Extracts. A nuclear extract of *E. aediculatus* cells was prepared as described previously (*15*). One mL of a 10-fold diluted extract was resolved on a HiPrep 16/60 Sephacryl S-300 HR column (Pharmacia, bed volume of 120 mL) run in nuclear extract buffer at 4 °C. Fractions of 1.5 mL were collected, and 10 μL of each fraction was analyzed by a telomerase activity assay and anti-p43 Western blot as described previously (*16*). For detection of RNA, 20 μL of each fraction was immobilized on nylon membranes by dot blotting (*35*) and analyzed by blot hybridization as described previously (*16*), using the following 5′-^{32}P-end-labeled DNA oligomers as probes: telomerase RNA, 5′-GGTTTTGGGGTTTTGCTTGACAG-3′; U6 snRNA, 5′-TCGCGCAGGGGCCATGCTAATCTTCTCT-3′; and 5S rRNA, 5′-CGCTTAACTTCGGAGTTCGGAAGGGATCCGGTGC-3′.

Immunoprecipitation and 3′-End Labeling of RNAs. E. aediculatus whole cell extract was prepared by sonicating cells in a buffer containing 50 mM Tris-HCl (pH 7.5), 10 mM $MgCl_2$, 200 mM NaCl, 0.1% Nonidet P-40, 1 mM dithiothreitol (DTT), and 10% (v/v) glycerol (5 mL of buffer/g of cell pellet) and clearing the lysate by centrifugation at 200000*g* for 2 h at 4 °C. Lysate (500 μL) was subjected to immunoprecipitation with 10 μL of anti-p43 antibody beads, followed by isolation of bound RNAs as described previously (*16*).

Two-fifths of the recovered RNAs were end-labeled at their 3′-termini in 10 μL reaction mixtures with 0.4 μM [α-^{32}P]cordycepin (5000 Ci/mmol) and 150 units of cloned yeast poly(A) polymerase (U.S. Biochemicals) in the manufacturer's buffer for 20 min at 30 °C. After removal of unincorporated label on G-25 spin columns (Roche), the RNAs were analyzed on 8% polyacrylamide sequencing gels containing 7 M urea and 1× TBE (×89 mM Tris, 89 mM boric acid, and 1 mM EDTA).

Expression of p43. To express p43 fused to an N-terminal FLAG epitope tag (Sigma), the *Nde*I−*Bam*HI fragment of pET15b p43 (*16*) was inserted into the *Nde*I−*Bgl*II sites of the pVLSG2-flag baculovirus transfer vector (generous gift from J. Goodrich, University of Colorado). Recombinant baculoviruses were generated by transfecting Sf9 cells with linearized wild-type baculovirus DNA and the transfer plasmid in Hink's TNM-FH medium at 27 °C according to standard protocols (*36*). Single recombinant viruses were isolated by a plaque assay from virus-containing cell supernatant obtained after 4 days. Viral stocks were amplified and titered. Recombinant p43 was expressed at 27 °C in 5 L oxygenated bioreactors by infecting 5×10^9 Sf9 cells with recombinant virus at a multiplicity of infection of 1 in 500 mL of medium for 1 h, followed by addition of 4.5 L of medium containing 10% fetal calf serum. Cells were harvested 48 h postinfection, washed twice with phosphate-buffered saline (PBS), and flash-frozen at −70 °C. Baculovirus procedures were carried out by the Tissue Culture Core Facility at the University of Colorado Cancer Center (Denver, CO).

Protein Purification. All following steps were carried out at 0−4 °C. For p43, insect cells (5−10 g) containing recombinant p43 were lysed by sonication in p43 buffer [50 mM Tris-HCl (pH 7.5), 0.5 M NaCl, 0.4% (v/v) Triton X-100, 1 mM DTT, and 10% (v/v) glycerol], supplemented with a protease inhibitor cocktail (Roche, Complete EDTA-free) and 0.1 mM phenylmethanesulfonyl fluoride (PMSF), using 5 mL of buffer/g of cells. The lysate was cleared by centrifugation at 100000*g* for 1 h, applied to a heparin−Sepharose column, and eluted with an NaCl gradient from 0.5 to 2 M in p43 buffer. p43 eluted between 1.0 and 1.2 M NaCl. Fractions containing p43 were pooled, adjusted to 0.5 M NaCl, and allowed to bind to anti-FLAG M2 antibody agarose affinity gel (Sigma) for 1 h, using 0.5 mL of gel/g of initial cell pellet. p43 was eluted by incubating the washed gel three times with 1 bed volume of 3× FLAG peptide (Sigma) at 250 μg/mL in p43 buffer for 1 h each. Purified p43 was concentrated by applying the pooled eluates to a 1 mL heparin column and eluting it with a step gradient from 0.5 to 2 M NaCl, followed by exhaustive dialysis against p43 buffer. Purified p43 was >95% homogeneous as assessed from gels stained with a fluorescent protein dye (SyproRed, Molecular Probes). Protein concentrations were determined by quantitating p43 band intensities on gels stained with SyproRed with a PhosphorImager, using a set of proteins at known concentrations as standards.

Expression and purification on recombinant yeast Lhp1p were carried out as described previously (*37*), except that the poly(U)−Sepharose purification step was omitted. Lhp1p was quantitated by a Bradford assay, using BSA as a standard.

Cloning of E. aediculatus RNA Genes. Genomic DNA was prepared from whole cells with a DNA extraction kit (Stratagene) and used as a template for PCR amplification of the genes for 5S rRNA and $tRNA^{Cys}$ with gene-specific primers and a primer that can anneal at the telomeres of all

macronuclear chromosomes (Telpr-1, 5′-$C_4A_4C_4A_4C_4$-3′), essentially as described previously (*24*). Primers FS-1F (5′-GCACCGGATCCCTTCCAACTCCGAAGTTAAGCG-3′) and FS-1R (5′-CGCTTAACTTCGGAGTTCGGAAGG-GATCCGGTGC-3′) were based on nucleotides 25−58 of the *Euplotes eurystomus* 5S rRNA sequence [GenBank entry X13718 (*38*)] and used to amplify the 3′- and 5′-portions of the *E. aediculatus* gene, respectively. Primers TC-1F (5′-ATAGCTCAGTGGTAGAGCA-3′) and TC-1R (5′-TGCTC-TACCACTGAGCTAT-3′) were based on nucleotides 7−25 of the *Euplotes octocarinatus* $tRNA^{Cys}$ sequence [GenBank entry Y17506 (*39*)] and used to amplify the 3′- and 5′-portions of the *E. aediculatus* gene, respectively. The sequences of the untranscribed gene regions were obtained from the PCR products and were employed to design primers for PCR amplification of the entire genes. Plasmids pEa5S and pEatRNACys were generated by amplifying the PCR products containing the 5S rRNA and tRNA genes, respectively, using primer pairs that facilitate runoff transcription of the genes by T7 RNA polymerase and cloned into pUC19, essentially as described previously (*15*) except that the 5′-primers did not contain a hammerhead ribozyme sequence. Primers were designed such that transcription would produce the natural RNA 5′-end (*38*, *39*), and both RNAs would end in a stretch of four U's.

These sequence data have been submitted to the DDBJ, EMBL, and GenBank databases as entries AY245017 ($tRNA^{Cys}$) and AY245018 (5S rRNA).

Design of Telomerase RNA Mutants. Plasmids encoding telomerase RNA mutants were produced by PCR mutagenesis, using the pEaT7 (*15*) or pEaNHT7 plasmid (*16*) as a template. Mutant RNAs are as follows (nucleotide positions based on ref *24*): Δ3′-U_4, Δ(186−189); Δ stem−loop IIIb, U79A/U81C; Δ stem−loop III, Δ(70−96); Δ stem−loop IVc, Δ(140−153,158−164); Δ stem−loop IVbc, Δ(135−153,158−170); Δ stem−loop IV, Δ(118−181); stem−loops I and IV, (13−99):GAAA; stem−loops I and IVab, (13−99):GAAA and Δ(140−153,158−164); and stem−loops I and IVa, (13−99):GAAA and Δ(135−153,158−170).

Binding Assays. Radiolabeled RNAs were prefolded in p43 buffer supplemented with 10 mM $MgCl_2$ and 200 μg/mL yeast tRNA by heating to 65 °C for 10 min and quick-cooling on ice. Dilutions of p43 were prepared in p43 buffer supplemented with 200 μg/mL BSA. Binding was initiated by combining equal volumes of the RNA and protein solutions (final concentration of radiolabeled RNA of 0.1−0.5 nM) and allowed to reach equilibrium by incubation on ice for 1 h. Complexes were resolved on 8% polyacrylamide (29:1 acrylamide:bisacrylamide ratio) gels containing 5% glycerol. Gels were run in 75 mM Tris and 75 mM glycine at 20 V/cm for 2.5 h at 16 °C with cooling coils. Using a PhosphorImager, amounts of bound and free RNA were determined for each p43 dilution, and the data were fitted by least-squares approximation to a two-state binding model using the program Kaleidagraph (Synergy Software). Average K_D values and standard deviations were calculated from three replicates of binding experiments.

Enzymatic Probing of the p43·Telomerase RNA Complex. Gel-purified 5′-end-labeled telomerase RNA at 5 nM was prefolded and allowed to bind to p43 at 1 μM as described above, except that the NaCl concentration was reduced to 100 mM and no BSA was added. Nuclease digestions were initiated by addition of 2 units of RNase T1 (U.S. Biochemicals), 0.02 unit of RNase V1 (Pharmacia), or 5 units of RNase T2 (Sigma) to 5 μL samples, and the reactions were allowed to proceed for 10 min on ice and stopped by addition of 15 μL of formamide loading buffer [95% formamide, 0.1× TBE, 5 mM EDTA, and bromophenol blue and xylene cyanol (0.01% each)]. Samples were resolved on 6 and 12% polyacrylamide gels containing 7 M urea and 1× TBE.

Cytology. An all-2′-*O*-methyl-RNA probe directed against nt 20−36 of telomerase RNA was synthesized by standard phosphoramidite chemistry with a 5′-amino modifier attached via a 12-carbon spacer. The oligomer was labeled postsynthesis with digoxigenin using a digoxigenin NHS-ester derivative (Roche), followed by reverse phase HPLC purification. Unless stated otherwise, all following steps were carried out at room temperature essentially as described previously (*40*). For in situ hybridization and FISH analysis, *E. aediculatus* nuclei were isolated by lysis of the cells with 1 mg/mL spermidine phosphate and 0.1% Triton X-100 and centrifugation at 1000*g* for 5 min (*41*). Nuclei were resuspended in Pringsheim medium [0.11 mM Na_2HPO_4, 0.08 mM $MgSO_4$, 0.85 mM $Ca(NO_3)_2$, and 0.35 mM KCl (pH 7.0)] containing 2% formaldehyde, incubated for 20 min at room temperature, and washed twice with Pringsheim medium. Nuclei suspensions were transferred to slides and dried overnight under vacuum. The slides were placed subsequently in ice-cold 70 and 95% ethanol for 5 min each and allowed to air-dry. Slides were washed twice with 2× SSC (1× SSC is 15 mM sodium citrate and 150 mM NaCl). For FISH analysis, hybridization was performed overnight in a humid chamber (Hybaid EasiSeal) in a volume of 65 μL with approximately 5 pmol of digoxigenin-labeled RNA probe/mL in 2× SSC at 42 °C. The slides were washed twice with 2× SSC and twice with 0.1× SSC at 42 °C, rinsed with PBS (2 min), and blocked in 1% blocking reagent (Roche) in PBS for 30 min. Slides were incubated with an anti-DIG rhodamine-conjugated antibody (Roche) at a dilution of 1:20 for 2 h in PBS and 1% blocking reagent, washed twice with PBS for 5 min each, and imaged. For in situ immunolocalization of p43, binding of anti-p43 antibodies to macronuclei was performed on the same slides as described above. The slides were washed twice with PBS for 15 min, followed by incubation with the rabbit anti-p43 antibody at a dilution of 1:25 in PBS and 1% blocking reagent for 2 h and blocking in PBS and 1% blocking reagent for 30 min. Slides were incubated with a pig anti-rabbit FITC-conjugated antibody (DAKO) for 2 h, washed several times with PBS, and imaged. Slides were imaged simultaneously for rhodamine and FITC with a Leitz DM RB microscope and detected with a Leica DC 300F camera.

RESULTS

Telomerase Is the Prevalent RNP Complex Containing p43 in Vivo. As a first step in determining whether p43 is present in macromolecular complexes other than telomerase, we subjected an *E. aediculatus* nuclear extract to gel filtration chromatography on a Sephacryl S-300 column. The column fractions were then analyzed by anti-p43 Western blot, dot-blot RNA hybridization, and telomerase activity assay. As shown in Figure 1, the vast majority of telomerase RNA coeluted with telomerase activity, consistent with previous observations indicating that most telomerase RNA is incor-

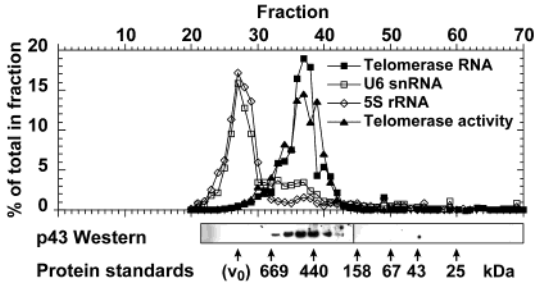

FIGURE 1: p43 protein from *E. aediculatus* nuclear extract cofractionates with telomerase on a gel filtration column. The quantities of telomerase RNA (■), U6 snRNA (□), 5S rRNA (◇), and telomerase activity (▲) present in each fraction were determined as described in Materials and Methods and plotted relative to the total amounts recovered. Western blots detecting p43 in the fractions and the elution positions of a set of protein molecular mass standards are shown below the plot. v_0 is the column void volume.

porated into the RNP enzyme (*15*). Significantly, p43 coeluted with telomerase, and no free p43 was detected, indicating that the majority of the nuclear p43 pool is contained in the telomerase RNP. In contrast, both U6 small nuclear RNA (U6 snRNA) and 5S ribosomal RNA (5S rRNA) eluted at a molecular mass position distinct from that of telomerase and near the exclusion volume of the column. These pol III transcripts are presumably incorporated in large snRNPs and ribosomal subunits, respectively.

On the basis of a calibration of the column with protein standards, we measured the apparent molecular mass of the telomerase complex to be 450−500 kDa. This is in contrast to a previous observation, where telomerase from nuclear extract was reported to sediment at 12.5 Sv, slightly faster than catalase [232 kDa/11.5 Sv (*15*)]. We do not know the reason for this discrepancy but note that the measurements presented here are in agreement with telomerase dimer formation, which has been suggested for the *Euplotes crassus* complex in vitro (*42*). Alternatively, our nuclear extract preparations may preserve additional telomerase-associated proteins in their telomerase-bound state.

Telomerase RNA Is the Prevalent RNA Species Associated with p43 in Vivo. Sizing column chromatography may not resolve telomerase from other RNPs of similar size. Similarly, the detection limit for p43 may not be sufficient for detection of small amounts of p43 present in other complexes, or these may have leaked out of the nuclei during isolation. We therefore tested whether other RNAs are associated with p43 in a whole cell lysate. Anti-La immunoprecipitates from human (*43*), yeast, and fruit fly (*44*) extracts have been shown to be enriched in pol III precursors, including pre-tRNAs and pre-5S rRNA. The presence or absence of these RNAs in anti-p43 immunoprecipitates from *E. aediculatus* extract therefore is expected to be a strong indication of whether p43 functions as a La protein or is a component of other RNPs. For these experiments, we chose to prepare the extract in a buffer with fairly low salt and detergent concentrations (200 mM NaCl and 0.1% NP-40 nonionic detergent), thereby ensuring that the stringency of our conditions was comparable to that used previously for anti-La immunoprecipitations (*43*, *44*).

As shown in Figure 2, the only RNA detected in anti-p43 immunoprecipitates was an RNA ~190 nt in length. Direct sequencing of this RNA with sequence-specific nucleases confirmed that it was telomerase RNA (data not shown). The

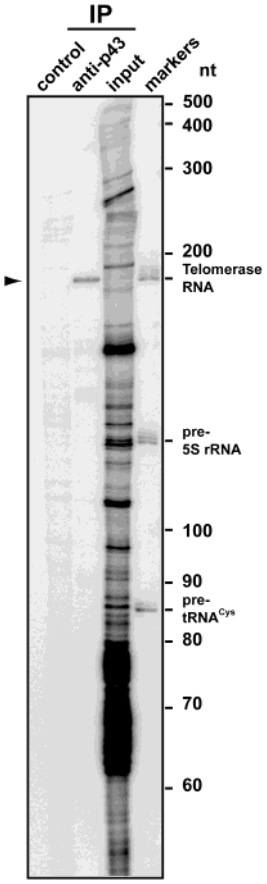

FIGURE 2: Telomerase RNA is the only detectable RNA that is associated with p43. *E. aediculatus* whole cell extract was subjected to immunoprecipitation (IP lanes) with preimmune antibody beads (control lane) or anti-p43 antibody beads (anti-p43 lane), followed by extraction of the RNAs, ^{32}P labeling at the 3′-end, and separation on a denaturing polyacrylamide gel. The input lane contains the labeled RNAs isolated from 1% of the extract used for immunoprecipitation. The markers lane shows in vitro-transcribed and 5′-^{32}P-end-labeled telomerase RNA, pre-5S rRNA, and pre-tRNA^{Cys}. The positions of RNA size standards are indicated on the right. An arrowhead highlights immunoprecipitated telomerase RNA.

antibody failed to enrich any other RNA present in the lysate. Specifically, the input extract, but not the immunoprecipitate, contained detectable amounts of RNAs that comigrated with *E. aediculatus* pre-tRNA or pre-5S ribosomal RNA markers (generated as described below), suggesting that such precursors were present in the extract but were not associated with p43. We conclude that p43 is primarily associated with telomerase RNA.

p43 Binds Telomerase RNA with Low-Nanomolar Affinity in Vitro. A more detailed analysis of this interaction in vitro required the use of recombinant p43. Previously, we showed that recombinant p43 expressed in *E. coli* UV cross-links to *E. aediculatus* telomerase RNA in the presence of excess nonspecific competitor RNAs (*16*), indicating that p43 binds telomerase RNA with some degree of specificity. However, p43 from this recombinant source was prone to aggregation under all conditions that were tested (data not shown). We therefore developed an alternative procedure for expressing and purifying p43, using baculovirus-infected insect cells. p43 was expressed N-terminally tagged with a FLAG epitope and purified from this source by heparin and antibody affinity chromatography (Figure 3A).

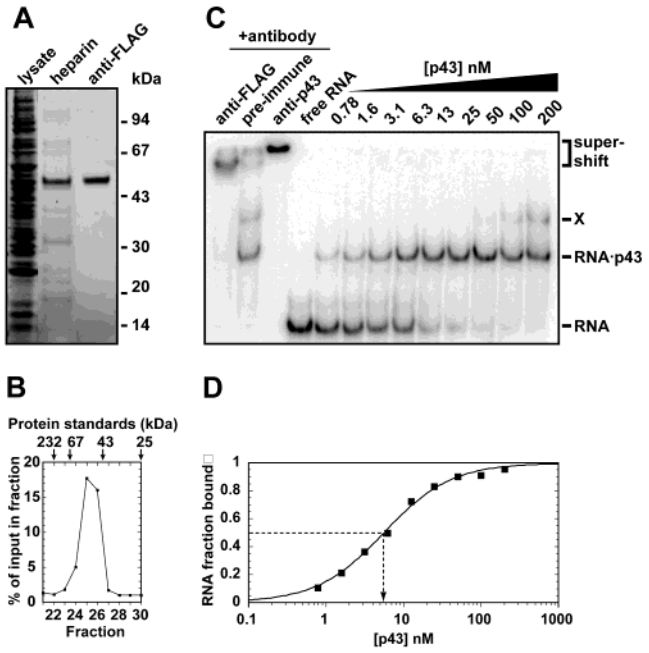

FIGURE 3: Recombinant p43 is largely monomeric and binds telomerase RNA in vitro. (A) Purification of p43 expressed recombinantly in insect cells. p43 tagged with the FLAG epitope at its N-terminus was purified to >95% homogeneity from an extract of baculovirus-infected insect cells (lysate lane) by purification on heparin−Sepharose beads (heparin) and anti-FLAG antibody agarose (anti-FLAG). Intact p43 is actually a 51 kDa protein, as described previously (*16*). Molecular mass standards are indicated on the right. (B) Size analysis of recombinant p43. Purified p43 was applied to a Superose-12 gel filtration column, and fractions were quantitatively analyzed for p43 by gel electrophoresis followed by protein staining with a fluorescent dye. The elution positions of a set of protein molecular mass standards are shown above the plot. (C) Electrophoretic mobility shift assay of the p43·telomerase RNA complex. Trace amounts of radiolabeled *E. aediculatus* telomerase RNA were incubated with p43 at the concentrations indicated above the lanes. For the lanes marked +antibody, samples contained p43 at 200 nM and the indicated antibodies. Complexes were separated on a nondenaturing polyacrylamide gel. The band marked X has not been characterized but presumably represents a complex of two p43 molecules per RNA molecule. (D) Quantitation of the binding data in panel C. Data are plotted as the fraction of RNA bound vs the protein concentration (■). The solid line is the least-squares fit to a two-state binding model.

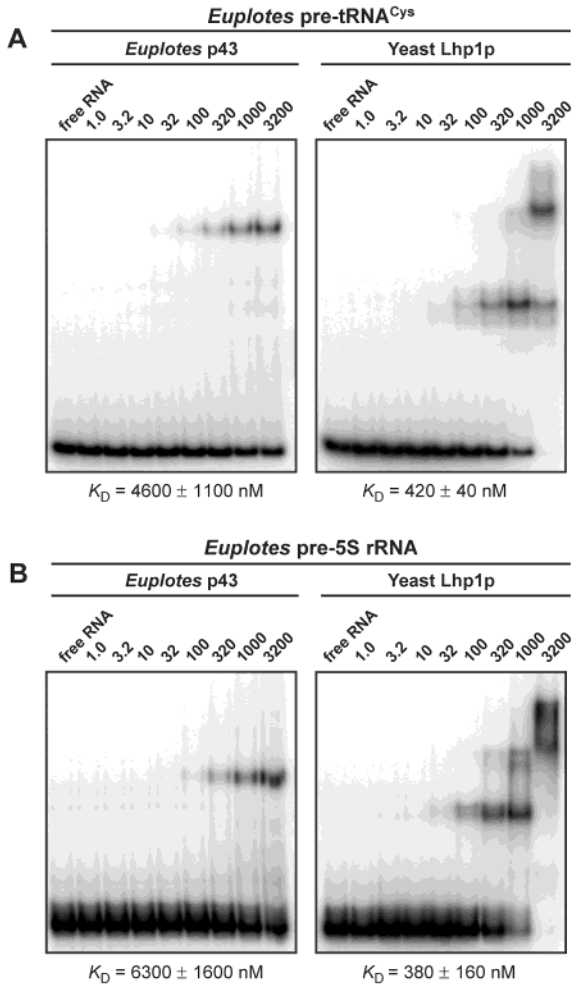

FIGURE 4: Pol III transcripts other than telomerase RNA are only weakly bound by p43. In vitro-transcribed *E. aediculatus* pre-tRNA^{Cys} (A) or pre-5S rRNA (B) was subjected to gel shift analysis using either *Euplotes* p43 (left panels) or the yeast La protein Lhp1p (right panels). Low-mobility complexes formed at high Lhp1p concentrations presumably represent binding of more than one Lhp1p molecule per RNA molecule. Protein concentrations in the binding reactions are given in nanomolar above each lane. The dissociation constants ± standard deviations determined from three replicates of binding experiments are given below the gels.

The elevated monovalent salt and nonionic detergent concentrations (500 mM NaCl and 0.4% NP-40, respectively) of the buffer used for purification were necessary to prevent aggregation of the recombinant protein (data not shown). Under these conditions, p43 behaved largely as a monomer as judged by gel filtration chromatography on a calibrated Superose-12 column (Figure 3B).

An electrophoretic mobility shift assay revealed that recombinant p43 binds telomerase RNA (Figure 3C). The observed shifted band was supershifted by both anti-p43 antibody and anti-FLAG antibody, but not by nonimmune IgG, indicating that the shifted complex contains p43. The interaction between p43 and telomerase RNA is specific because binding was observed in the presence of 100 μg/mL yeast tRNA, which is a component of the binding buffer, but excess unlabeled telomerase RNA competed with the band shift (data not shown). The binding interaction fit a two-state binding model well (Figure 3D) and gave an apparent dissociation constant (K_D) of ~5 nM in this experiment; more precise repeated measurements gave a K_D of 2.9 ± 0.4 nM (Figure 5A, left panel).

p43 Does Not Bind Strongly to Pre-tRNA and Pre-5S rRNA in Vitro. We began to address p43's specificity of RNA recognition by testing several RNAs for binding. In light of the observed La homology, we examined additional *Euplotes* pol III transcripts. The database contained several entries for genes transcribed by pol III from other *Euplotes* species, and these genes are usually highly conserved. However, we were concerned that using these heterologous RNAs in p43 binding assays could produce negative results due to less conserved residues that may be important for binding, especially in the less conserved 5′-leader and 3′-trailer sequences. We therefore cloned two *E. aediculatus* macronuclear chromosomes encoding pol III transcripts by a PCR-based approach (see Materials and Methods): the gene for a tRNA^{Cys} isoacceptor (tRNA$^{Cys}_{GCA}$), using sequence information from *E. octocarinatus* (*39*), and the gene for 5S rRNA, using sequence information from *E. eurystomus* (*38*). While the coding regions of *E. aediculatus* and *E. octocarinatus* 5S rRNA were

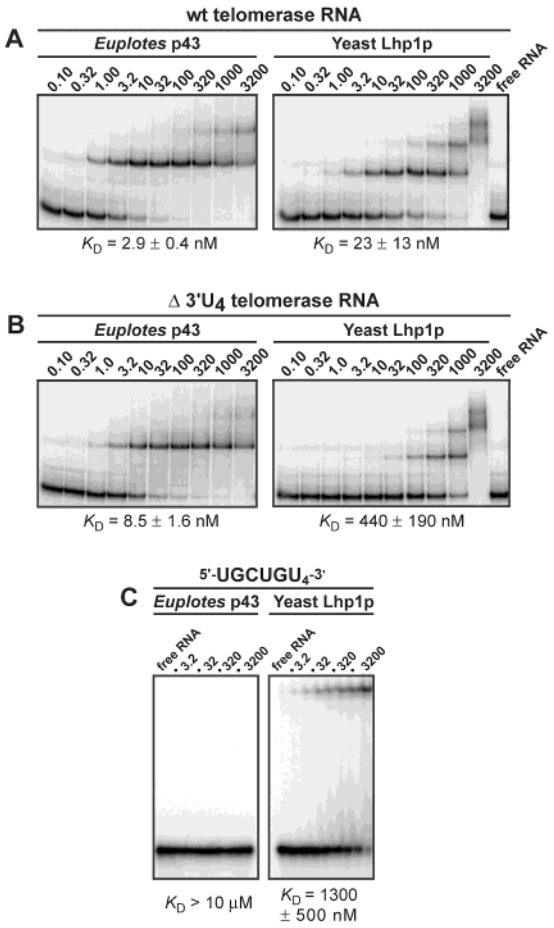

FIGURE 5: 3′-Terminal U residues are not critical for p43 binding. In vitro-transcribed wild-type *E. aediculatus* telomerase RNA (A), a mutant version of telomerase RNA lacking its oligo-U tail (B), or a synthetic nonanucleotide RNA ending in four U residues (C) was subjected to gel shift analysis using either *Euplotes* p43 (left panels) or yeast Lhp1p (right panels).

100% identical, we found one nucleotide change each in the 5′-leader and 3′-trailer between *E. aediculatus* and *E. eurystomus* $tRNA^{Cys}$.

These RNAs were transcribed in vitro in their precursor forms with T7 RNA polymerase and examined for binding to p43 by a gel shift assay. The use of recombinant yeast La protein Lhp1p (*37*, *44*) in parallel assays as a control allowed direct comparison of the results obtained for p43 with those of an authentic and well-characterized La protein. Figure 4A shows our data for binding of p43 and Lhp1p to *E. aediculatus* pre-$tRNA^{Cys}$. While p43 gave primarily a single gel shift complex, Lhp1p gave additional low-mobility complexes at high protein concentrations that presumably represent two or more Lhp1p molecules bound to a single RNA. p43 bound this tRNA with a K_D of 4.6 μM, but Lhp1p bound it with a K_D of 420 nM, an approximately 11-fold higher affinity.

Similar results were obtained for pre-5S rRNA as the binding substrate (Figure 4B). Here, the respective K_D values were determined to be 6.3 μM for this RNA's interaction with p43 and 380 nM for its interaction with Lhp1p. Thus, Lhp1p bound *Euplotes* 5S rRNA approximately 17-fold more tightly than did p43. The difference in RNA binding affinities observed between these proteins is not due to a generally lower affinity of p43 versus Lhp1p, since Lhp1p bound telomerase RNA with a K_D of 23 nM (Figure 5A, right panel) and thus 8-fold more weakly than the value of 2.9 nM measured for the p43−telomerase RNA interaction (Figure 5A, left panel). In summary, these data suggest that p43 specifically recognizes telomerase RNA and discount p43 as the *Euplotes* La protein.

3′-Uridylates Are Not an Important Binding Determinant for p43. La proteins specifically recognize the run of uridylates present at the 3′-end of all primary pol III transcripts (*29*, *30*). It was therefore important to see how well p43 would bind a mutant of telomerase RNA whose 3′-run of U's was deleted. Figure 5A shows that p43's affinity for this mutant (K_D = 8.5 nM) was reduced by only 3-fold compared to that of wild-type RNA. In contrast, Lhp1p's affinity (K_D = 440 nM) dropped ∼20-fold when these residues were removed. This indicates that the presence of a 3′-terminal stretch of U's, the hallmark of pol III transcripts, is much less critical for p43 binding than for La protein binding. This notion was confirmed by testing the affinities of binding of p43 and Lhp1p to a synthetic RNA nonamer ending in four U's (*45*). As Figure 5C shows, no binding was detected for p43 at concentrations of up to 3.6 μM, whereas Lhp1p1 bound the oligomer with a K_D of ∼1.3 μM. Thus, even outside the context of a large RNA molecule, p43's binding to uridylates is comparably weak.

Footprinting of the RNA−Protein Complex Points to a Central Region of RNA Binding. The experiments described above clearly indicated that p43 recognizes structural elements in telomerase RNA other than the 3′-uridylates. To directly determine which region(s) of the RNA is in contact with the protein or is structurally changed by bound protein, we performed enzymatic footprinting of p43-bound telomerase RNA (for a review, see ref *46*). This method exploits the fact that due to steric hindrance, RNases cannot access a region of an RNA molecule that is bound by a protein, resulting in a reduction in the level of nuclease cleavage at that site. Alternatively, a change in RNA cleavage in the presence of bound protein can stem from an indirect effect. The protein induces changes in the structure of the RNA beyond its immediate binding site, which leads to a reduction or an enhancement of the accessibility and/or reactivity of the RNA site toward a given RNase.

We chose to use two single-strand-specific RNases (RNase T1, cleaving at the 3′-side of G residues, and RNase T2, cleaving at the 3′-side of all four nucleotides) and the double-strand-specific RNase V1 (cleaving helical or stacked residues without sequence preference) to probe the structure of telomerase RNA in the presence or absence of bound p43. To this end, the RNA was in vitro transcribed, end labeled, and folded, followed by incubation with p43 or heat-denatured p43 and digestion with the indicated RNase (Figure 6A). Inspection of the RNase cleavage pattern of the RNA without p43 bound to it (lanes indicated with −) largely confirms the *Euplotes* telomerase RNA secondary structure model (Figure 6B), which was built on comparative sequence analysis (*24*). Helical regions I and IV (Figure 6A, left panel; helical stems indicated by vertical bars next to the gels) were generally susceptible to digestion by RNase V1, whereas the interspersed non-base-paired regions tended to be cleaved by RNases T1 and T2. Parts of the region between nucleotides 13 and 69, although not constrained to be double-stranded by phylogeny (right panel), are cleaved by RNase

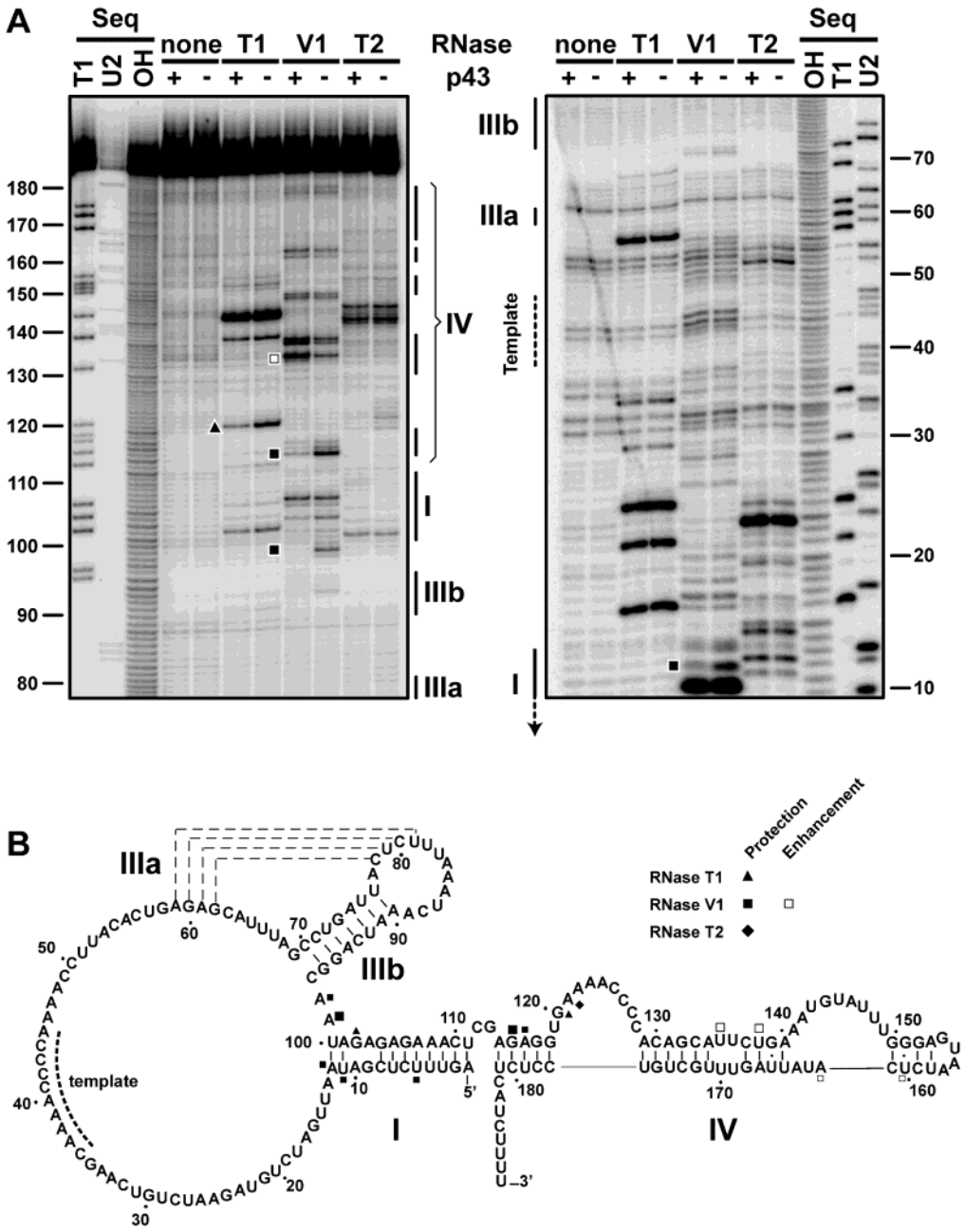

FIGURE 6: The footprinting experiment shows that p43 protects a central portion of telomerase RNA from nucleolytic digestion. (A) Samples containing 5′-^{32}P-labeled telomerase RNA were incubated with either p43 (+ lanes) or heat-denatured p43 (− lanes), followed by either no treatment (none) or digestion with the indicated RNases. The Seq lanes contained sequence markers generated by incubation of denatured telomerase RNA with either RNase T1 (T1, cleavage at G residues), RNase U2 (U2, cleavage at A residues), or alkali (OH, cleavage at all residues). Symbols next to gel bands show some of the most obvious footprints (filled symbols) or enhancements of cleavage (empty symbols) upon protein binding. RNA fragments were extracted and resolved on denaturing 6% (left) or 12% (right) polyacrylamide gels. Nucleotide positions, the location of secondary structure elements (roman numerals), and the template region are shown next to the gels. (B) Superposition of the results from panel A on the secondary structure model of *E. aediculatus* telomerase RNA (*24*). Solid symbols indicate protection from digestion by RNase T1 (▲), RNase V1 (■), and RNase T2 (◆) in the presence of p43, while empty symbols indicate enhancement of cleavage in the presence of p43, observed only for RNase V1 (□). The size of the symbol reflects the difference in band intensities between the corresponding + and − lanes, as judged by visual inspection of the gels.

V1. This is consistent with previous biochemical evidence from *Tetrahymena* indicating that this domain of telomerase RNA is generally single-stranded but contains regions that are constrained into an ordered conformation (*47*−*49*). Likewise, we did not observe footprinting patterns that indicate the stable formation of helical region IIIa or -b. This is not unexpected, as this domain of telomerase RNA has been observed to be dynamic when not bound by TERT in both *Tetrahymena* (*47*, *49*) and humans (*50*). We conclude that *Euplotes* telomerase RNA is unlikely to be grossly misfolded under our conditions, but instead assumes a secondary structure closely related to that supported by phylogenetic and biochemical evidence.

In the presence of bound p43 (Figure 6A, lanes marked with +), the changes in the RNase cleavage patterns did not indicate large structural RNA rearrangements or expansive regions of protein binding. Instead, a few distinct changes in RNase cleavage were seen. Specifically, residues U5, U11,

A12, A98, A99, G115, and A116 became protected from cleavage by RNase V1, G102 and G120 from cleavage by RNase T1, and residue A122 from cleavage by RNase T2. In contrast, residues U135, U138, U160, and A162 all exhibited enhancements in cleavage by RNase V1. Superposition of these observations on the secondary structure model of the RNA [Figure 6B (*24*)] reveals that these changes are clustered. The protections are localized to stem I and the adjacent (proximal) part of stem IV, while enhancements are exclusively located in the central and distal parts of stem IV. Encouraged by the striking clustering of the observed changes, we favor a straightforward interpretation of these results which contends that p43 binds at or near stem I and induces a conformational change of the more distal parts of stem IV without contacting them. This structural rearrangement in stem IV could be an increase in helical character or a change in the three-dimensional positioning of this helix within the entire RNA molecule, leading to increased accessibility to RNase V1.

Binding Constants for Binding of Telomerase RNA Mutants to p43 Point to a Central RNA Region Important for Binding. Further evidence that a distinct region within the core of the telomerase RNA molecule is bound by p43 comes from measurements of the affinity of a variety of truncation, deletion, and disruption mutants of this RNA. These mutants were generated by PCR, subcloned, in vitro transcribed, and tested for p43 binding by our standard gel shift assay. Figure 7 summarizes these results, with the RNA mutant structures rendered as stick diagrams and the measured K_D values given below each RNA construct. Figure 7A recapitulates our results for the wild-type RNA (top panel) and the 3′-U_4 deletion construct (bottom panel) for comparison and shows how we have, for the purpose of this paper, subdivided the long stem IV into parts a−c.

When the stem IIIb pseudoknot interaction was disrupted by mutating two nucleotides, a modest increase in K_D of 4−5-fold compared to that of the wild type was observed (Figure 7B, top panel). Removal of the entire stem−loop III had a similar effect (bottom panel). These observations suggest that stem−loop III is not critical for p43 binding. However, its presence contributes a moderate stabilization of the RNA−protein interaction, possibly by stabilizing the overall fold of the RNA.

Gradual shortening of stem IV by deleting either its distal end (Figure 7C, top panel) or its distal and central portions (middle panel) did not result in a significant change in K_D despite the loss of nucleotides that show enhancement of nucleolytic digestion in our footprinting assays. This strongly suggests that these portions of the RNA, although evidently undergoing a conformational change upon p43 binding, are not contacted by the protein. However, when almost the entire stem−loop IV was removed (bottom panel), together with several nucleotides that are protected from nuclease digestion (including the strongly protected G115), the K_D increased ∼40-fold, consistent with the idea that p43 binds at or near the proximal portion of stem IV.

When we removed the entire "central wheel" and stem−loop III and replaced these structures with a GAAA tetraloop, we saw a loss of binding affinity of ∼20-fold. This reduction in binding probably occurs because part of the p43 binding site, which comprises some of the protected nucleotides (including the strongly protected A99), has been lost. In contrast to the results from mutants with an intact central wheel and stem−loop III (Figure 7C), here, additional shortening of stem IV resulted in a further weakening of p43 binding, albeit by only 2−3-fold. In summary, these data confirm the footprinting results and point to stem I and adjacent portions of the RNA as the primary binding site for p43.

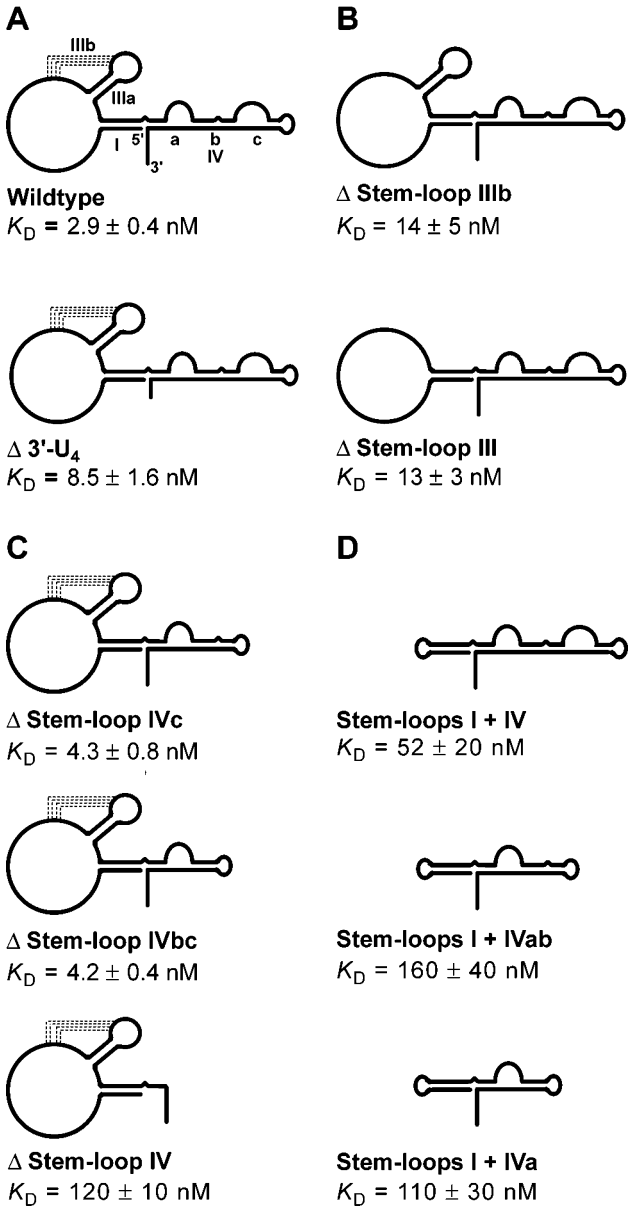

FIGURE 7: Equilibrium dissociation constants of telomerase RNA truncation and disruption mutants point to a central region that is important for p43 binding. RNA variants were generated as described in Materials and Methods. K_D values for mutant RNAs were quantitated by a gel shift assay and are given with the standard deviations determined from three replicates of binding experiments. (A) Wild-type (top) and telomerase RNA with its 3′-U's deleted (bottom). (B) Disruption of the stem−loop IIIb pseudoknot interaction (top) and deletion of stem−loop III (bottom). (C) Deletion of region c (top) and regions b and c (middle) of stem−loop IV, and of the entire stem−loop IV (bottom). (D) Deletion constructs lacking the entire central wheel, having an intact stem−loop IV (top) and the stem-loop IV truncations (middle and bottom) described in the top and middle parts of panel C, respectively.

p43 Binds Tetrahymena Telomerase RNA. Pairwise comparison of telomerase RNA primary sequences from seven hypotrichous ciliates (such as *Euplotes*, *Oxytricha*, and

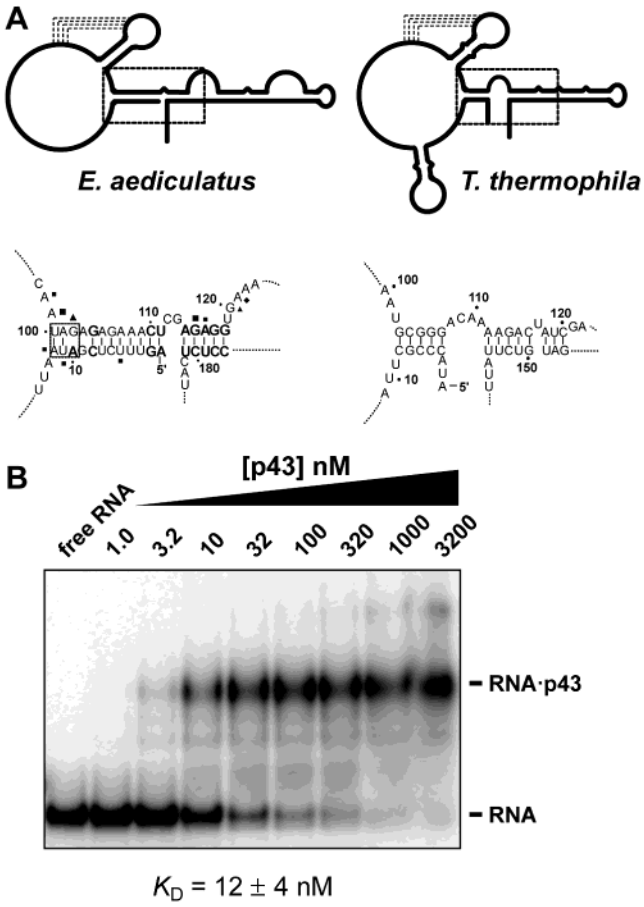

FIGURE 8: *Euplotes* p43 binds *Tetrahymena* telomerase RNA. (A) Secondary structure models of *E. aediculatus* (left) and *T. thermophila* (right) telomerase RNAs. Close-ups of the boxed RNA regions have nuclease footprinting results from Figure 6 superimposed. In the left panel, nucleotides conserved in hypotrichous ciliates (*24*) are shown in bold letters and nucleotides invariant in *Euplotes* species are boxed. (B) Gel shift assay of the complex between p43 and *T. thermophila* telomerase RNA. The dissociation constant ± standard deviation determined from three replicates of binding experiments is stated below the gel.

Stylonychia) revealed that these RNAs have diverged substantially, having as little as 50% nucleotide conservation (*24*). Overall, the region of proposed p43 binding shows a low degree of conservation among hypotrichs, similar to that of the entire RNA (*24*). However, as shown in Figure 8A (left panel), the sequence of the proximal portion of stem IV is invariant among the hypotrichs (*24*). Likewise, the two base pairs at the base of stem I (boxed in the sequence shown in Figure 8A) are invariant in the three *Euplotes* species that have been examined (*24*). Phylogenetic evidence therefore does not provide any clues as to whether the p43−RNA interaction might be predominantly sequence- or structure-specific. We therefore tested whether p43 is capable of binding telomerase RNA from the holotrichous ciliate *Tetrahymena thermophila*, as this RNA has a secondary structure similar to that of hypotrichs (Figure 8A, top diagrams) but no sequence conservation [Figure 8A, bottom diagrams (*24*)]. As shown in Figure 8B, this RNA was bound by p43 with an affinity constant (K_D = 12 nM) only 4-fold reduced compared to that of the cognate interaction, suggesting that p43 recognizes telomerase RNA primarily by its structure, rather than its primary sequence.

p43 Largely Colocalizes with Telomerase RNA in Isolated E. aediculatus Macronuclei. The relative spatial distribution of p43 and telomerase RNA was studied by indirect immunofluorescent antibody staining and fluorescence in situ hybridization (FISH) of fixed macronuclei, respectively, followed by imaging by confocal microscopy (Figure 9). Ciliates have two kinds of nuclei in a single cell: a micronucleus containing the diploid germline DNA and a polyploid macronucleus in which most of the cell's RNA synthesis occurs (for a review, see ref *51*); the latter is a worm-shaped organelle in *Euplotes*. p43 had a nonuniformly distributed staining pattern in the macronucleus, with the majority of signal localized to discrete foci (Figure 9A). The nucleus shown in Figure 9 was in S phase, as is indicated by the presence of the so-called replication band (arrowheads in Figure 9), the site of DNA replication in hypotrichous ciliates (for reviews, see refs *51* and *52*). More intense p43 staining was observed at this structure, indicating that at the replication band, p43 is enriched, more accessible to the antibody, or both. In interphase nuclei, the discrete foci persisted (data not shown), indicating that the intranuclear distribution of the majority of p43 is not cell cycle-dependent.

When the nuclei were imaged simultaneously for telomerase RNA, a staining pattern very similar to that of p43 was observed (Figure 9B). The telomerase RNA signal, as observed previously (*53*), was concentrated in discrete foci and the replication band; in our preparations, additional disperse staining throughout the nucleus was observed as well. Since this latter staining had not been observed previously, we presume this was nonspecific background staining caused by the less stringent hybridization conditions employed in the experiments presented here. Superposition of the p43 and telomerase RNA staining patterns (Figure 9C) revealed that p43 and telomerase RNA largely colocalize in the replication band and in the foci, although the relative intensities of the two signals at any given focus were generally not identical. This may indicate that the relative concentrations of p43 and telomerase RNA and/or accessibilities to the probes vary at the foci. Alternatively, the dose−response curves for staining of p43 and telomerase RNA might be very different. However, no staining was seen when nuclei were incubated only with secondary antibodies. In addition, no FISH signal was observed when the nuclei were digested with RNase A prior to staining or when an all-2′-*O*-methyl-RNA of arbitrary unrelated sequence was used as a probe (data not shown). We conclude that p43 and telomerase colocalize at the probable site of telomerase action, i.e., the replication band, and exhibit similar but nonidentical distributions throughout the macronucleus.

DISCUSSION

The maturation pathways of yeast and vertebrate telomerase are distinct but involve conserved proteins that also function in the maturation of other RNPs. Thus, the hypothesis that ciliates, with their pol III-transcribed telomerase RNAs, employ a maturation pathway involving the conserved La protein appeared to be attractive. However, in this paper, we show that none of the biochemical properties of p43 that we tested are reminiscent of a La protein but, instead, p43 has the character of a telomerase-specific protein. While the precise function of this telomerase subunit remains to be investigated, the presence of the conserved

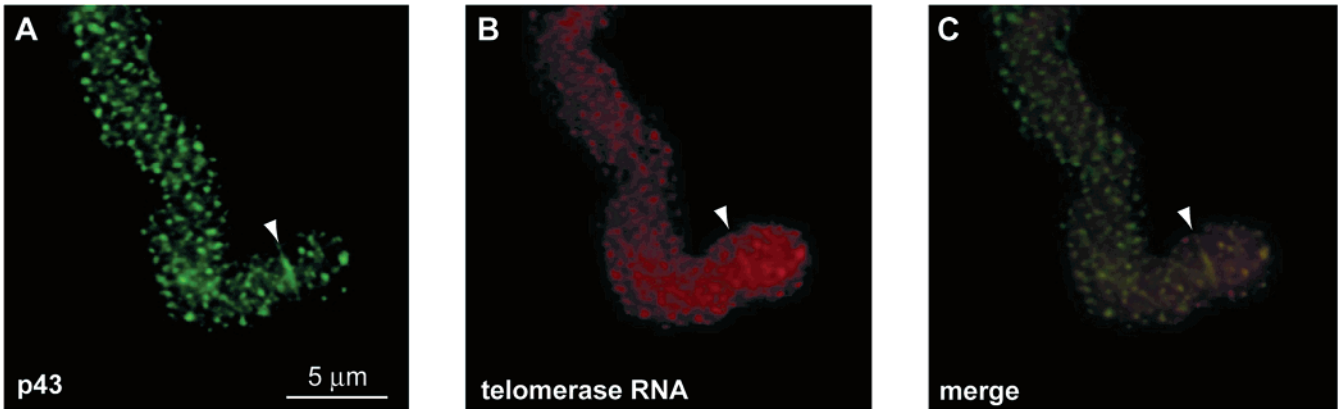

FIGURE 9: p43 largely colocalizes with telomerase in vivo. *E. aediculatus* macronuclei were isolated, fixed, and stained for p43 by in situ immunofluorescence, using a polyclonal antibody against p43 and a FITC-conjugated secondary antibody. Telomerase RNA was detected by FISH using a digoxigenin-conjugated oligonucleotide probe and a rhodamine-conjugated anti-digoxigenin antibody. p43 (A) and telomerase RNA (B) were imaged simultaneously. (C) Superposition of panels A and B. Arrowheads point to the replication band. The scale bar is 5 μm.

La sequence motif in p43 and the experiments presented here may provide a clue.

Association of p43 Primarily with Telomerase. Biochemical fractionation of nuclear extract and anti-p43 immunoprecipitation of RNAs from whole cell extract both gave no indication that p43 is in a complex with any RNP other than telomerase. While we cannot rule out the possibility that steady-state levels of pol III RNA transcript precursors are unusually low in *Euplotes* cells, thus precluding detection of p43-associated pools of such RNAs, it is clear that the vast majority, and perhaps all, of p43 in the cell is associated with telomerase. Attempts to design probes that would specifically detect precursor RNAs failed because the 3′-trailers of both pre-tRNA$^{Cys}_{GCA}$ and pre-5S rRNA are too short and largely composed of U's, providing insufficient discrimination (data not shown).

Under the conditions of high stringency employed for in vitro binding experiments, p43 discriminates between telomerase and other pol III transcripts by a factor of at least ~1500-fold, while showing an only ~3-fold dependence of binding affinity on the 3′-U tail of telomerase RNA. This contrasts starkly with Lhp1p, whose affinity for other pol III transcripts is reduced only ~15−20-fold compared to that of telomerase RNA, but shows a discrimination of ~20-fold for the 3′-U tail. It is unclear why, under these conditions, Lhp1p binds telomerase RNA more tightly than pre-tRNA and pre-5S rRNA. However, under the lower-stringency conditions used for Lhp1p binding assays (*54*), these RNAs show more similar K_D values (2.6 ± 0.4 nM for telomerase RNA, 6.3 ± 1 nM for pre-tRNA, and 5.2 ± 1.1 nM for pre-5S rRNA), while no significant change is seen for p43 (data not shown).

Specific Recognition of Ciliate Telomerase RNA Structure. Our results from footprinting of the telomerase RNA·p43 complex and from analysis of p43 binding to telomerase RNA mutants are consistent with a model in which p43 binds to stem I and adjacent regions of telomerase RNA, with concomitant conformational changes at more distant parts of stem IV. While this method of structural probing did not allow examination of the pseudoknot region and the very 3′-end of the RNA, mutants lacking these RNA regions did not show severely reduced p43 binding, and therefore, they cannot contribute much to the interaction. Stabilization of several RNA regions, including the pseudoknot, is observed upon binding of TERT in *Tetrahymena* (*49*); in *Euplotes*, such TERT-induced structural rearrangements may therefore create p43 binding sites that are only observed in the ternary complex.

Our findings assign a specific biochemical role, that of serving as a protein binding site, to stem I and adjacent nucleotides of telomerase RNA. Stem I, a long-range base pairing interaction, is not essential for in vitro function of human telomerase (*55*, *56*) but is conserved in ciliates and most vertebrates (*3*), suggesting that this helix may serve an in vivo function. Human La has been reported to UV cross-link to in vitro-transcribed telomerase RNA in extracts, and cross-linking was abolished in the presence of an oligonucleotide directed against the 5′-strand of the helix (*57*). Consistent with protein binding to the RNA in this region, footprinting experiments in human cell extracts show that this portion of telomerase RNA is largely protected from nuclease digestion and chemical modification, compared to the naked RNA (*50*). In human, the La protein may therefore bind telomerase RNA at a site that is structurally equivalent to the p43 binding site in *Euplotes*. However, only a minor fraction of the input telomerase activity was recovered in anti-La immunoprecipitates from human cell extracts (*57*), suggesting that a different protein may contribute to much of the observed RNA protection. Thus, unlike the case in *Euplotes*, in human cells only a minority of active telomerase RNPs may be associated with La, and it remains to be seen whether p43 and La serve similar functions in these organisms.

The putative RNA binding site of p43 is distinct from, and does not overlap with, the RNA structural elements required for TERT binding in *Tetrahymena* (*9*, *49*), consistent with the finding that both proteins are in the same complex in *Euplotes* (*15*). Interestingly, TERT binding to *Tetrahymena* telomerase RNA results in protection of stem IV from RNase V1 digestion (*49*), despite the minor role of this helix in direct TERT binding (*9*). This observation was interpreted as a conformational change induced by TERT (*49*). In contrast, p43 binding has the opposite effect, i.e., enhancement of cleavage by this double-strand-specific nuclease, suggesting that p43 perhaps counteracts a TERT-induced perturbation in parts of this helix.

Despite the lack of primary sequence conservation between the *Euplotes* and *Tetrahymena* telomerase RNAs, both are bound by p43 with an only 4-fold difference in binding affinity. This finding indicates that RNA recognition by p43 is largely governed by secondary and/or tertiary structure, rather than by primary nucleotide sequence. However, p43 cannot simply be a nonspecific dsRNA-binding protein because it does not bind to the P4−P6 domain of the *Tetrahymena* group I intron ribozyme (*16*), pre-tRNA, or pre-5S rRNA (this work), all of which contain helical regions. In ciliate telomerase RNAs, stem I and the proximal portion of stem IV invariably are uninterrupted helices and thus by themselves provide no plausible structure determinants for specific protein binding. (The noncanonical $G_9 \cdot A_{103}$ $A_{10} \cdot G_{102}$ tandem pairs present in the *E. aediculatus* RNA, common base oppositions in RNAs, are not conserved among *Euplotes* species and thus are unlikely to act as specific protein binding sites.) In contrast, the single-stranded residues near the base of stem I, the junction between stems I and IV, and the bulge in the proximal part of stem IV are more likely candidates for protein recognition sites. These are present in all ciliates, but their lengths and relative positioning are not conserved. Interestingly, a conserved and functionally critical GA bulge found in the middle of stem IV of *Tetrahymena* telomerase RNA shows strong DMS modification in vitro but not in vivo, perhaps indicating that the bulge serves as a binding site for a p43 homologue (*48*).

Colocalization with Telomerase. Immunolocalization revealed that p43 localizes to specific subnuclear structures. In contrast, anti-La immunofluorescence staining experiments in organisms ranging from yeast (*54*) to humans (*43*) did not give any indication of a nonuniform subnuclear distribution of the La protein. Instead, La showed both nucleolar and nucleoplasmic staining. *Euplotes* p43 is present in the replication band and thus colocalizes with telomerase at this putative site of telomerase action. This result highlights previous biochemical evidence indicating that p43 is part of the active telomerase complex (*15*, *16*). In addition, p43 colocalizes with telomerase RNA at previously observed telomerase foci; since these foci do not stain for telomeres, they are unlikely to be sites of telomerase action (*53*). It has been speculated that, given their large size and number, the observed foci are not dedicated to telomerase but instead may be related to the Cajal (coiled) bodies and interchromatin granule clusters (ICGs) of animal and plant nuclei (*53*). The function of these highly dynamic structures is still not clear, but evidence that they may be sites of storage and preassembly of protein components into particles that are involved in transcription and processing (such as splicing, capping, and 3′-end processing) of a variety of RNAs has been accumulating (for reviews, see refs *58* and *59*). Human telomerase RNA (*2*, *60*) and TERT (*61*) independently localize to the nucleolus. Furthermore, recent studies suggest that both the RNA (*6*, *62*) and TERT (*63*) may also pass through Cajal bodies. Enhanced release of the telomerase complex to the nucleoplasm from nucleolar sequestration has been observed at the expected time of telomere replication (*64*). Thus, the human telomerase RNP may be assembled and/or stored at these intranuclear sites and reach the telomere by a subnuclear shuttling mechanism. The fact that p43 is observed at both telomere-negative foci and at the telomere-containing replication band suggests that the spatial separation between telomerase assembly and storage on one hand and telomerase action on the other may be conserved between ciliates and vertebrates.

A Telomerase-Specific La-Motif Protein. p43 has properties of a telomerase-specific factor, yet it shares a structural feature, the La motif, with the less specialized La protein. The function of this sequence motif remains unclear, but evidence suggests that it is involved in RNA binding. While the isolated La motif does not bind RNA, small deletions within the motif in the context of the full-length protein result in a strong reduction in RNA binding affinity (*65*, *66*). Moreover, the La motif has been proposed to form an RRM (*67*). Genes encoding proteins that contain a La motif but are otherwise unrelated to authentic La proteins have been found in a variety of eukaryotic genomes (*28*, *68*). Sequence analysis revealed that their La motifs are generally more similar to each other than to those of La proteins, and several families of these La motif-containing proteins can be distinguished (*28*, *68*). However, a recent phylogenetic analysis did not clearly group p43 into any of these families (*28*). While the role of most La motif proteins is unknown, the two related yeast La motif proteins Slf1p and Sro9p have been shown to be RNA-binding proteins associated with polyribosomes and may function in mRNA stability or translation (*68*). Thus, these proteins may also serve a more specialized role.

It is tempting to speculate that p43 fulfills functions in the telomerase complex similar to those proposed for authentic La proteins, and such functional conservation may be mediated by the La motif. La proteins have been proposed to confer nuclear localization to RNPs (*29*, *31*, *69*, *70*). Since telomerase functions in the nucleus, p43 may act as a nuclear retention factor for telomerase. Likewise, binding of the yeast La protein Lhp1p to pre-tRNAs has been proposed to promote RNA conformations that favor productive processing of these transcripts; thus, p43 may act as a molecular chaperone for RNAs (*32*, *37*). p43 may similarly act to stabilize the structure of telomerase RNA, consistent with our observation that p43 may affect the structure of portions of the RNA not in direct contact with the protein. Further insight into the function of p43 in telomerase may be gained from in vivo studies and in vitro reconstitution of active *Euplotes* telomerase from recombinant components, as has been achieved for the mammalian (*55*) and *Tetrahymena* (*71*) complexes.

ACKNOWLEDGMENT

We thank Kurt Christensen from the Tissue Culture Core Facility at the University of Colorado Cancer Center for baculovirus and protein production, J. Kloetzel for the gift of *E. aediculatus* strains, and S. Wolin for the gift of the Lhp1p expression plasmid. S.A. is grateful to A. Berglund, T. Bryan, A. Seto, and S. Wolin for helpful discussions.

REFERENCES

1. Seto, A. G., Zaug, A. J., Sobel, S. G., Wolin, S. L., and Cech, T. R. (1999) *Nature 401*, 177−180.
2. Mitchell, J. R., Cheng, J., and Collins, K. (1999) *Mol. Cell. Biol. 19*, 567−576.
3. Chen, J.-L., Blasco, M. A., and Greider, C. W. (2000) *Cell 100*, 503−514.
4. Mitchell, J. R., Wood, E., and Collins, K. (1999) *Nature 402*, 551−555.

5. Dragon, F., Pogacic, V., and Filipowicz, W. (2000) *Mol. Cell. Biol. 20*, 3037−3048.
6. Pogacic, V., Dragon, F., and Filipowicz, W. (2000) *Mol. Cell. Biol. 20*, 9028−9040.
7. Holt, S. E., Aisner, D. L., Baur, J., Tesmer, V. M., Dy, M., Ouellette, M., Trager, J. B., Morin, G. B., Toft, D. O., Shay, J. W., Wright, W. E., and White, M. A. (1999) *Genes Dev. 13*, 817−826.
8. Forsythe, H. L., Jarvis, J. L., Turner, J. W., Elmore, L. W., and Holt, S. E. (2001) *J. Biol. Chem. 276*, 15571−15574.
9. Licht, J. D., and Collins, K. (1999) *Genes Dev. 13*, 1116−1125.
10. Lundblad, V., and Szostak, J. W. (1989) *Cell 57*, 633−643.
11. Lendvay, T. S., Morris, D. K., Sah, J., Balasubramanian, B., and Lundblad, V. (1996) *Genetics 144*, 1399−1412.
12. Seto, A. G., Livengood, A. J., Tzfati, Y., Blackburn, E. H., and Cech, T. R. (2002) *Genes Dev. 16*, 2800−2812.
13. Evans, S. K., and Lundblad, V. (1999) *Science 286*, 117−120.
14. Taggart, A. K., Teng, S. C., and Zakian, V. A. (2002) *Science 297*, 1023−1026.
15. Lingner, J., and Cech, T. R. (1996) *Proc. Natl. Acad. Sci. U.S.A. 93*, 10712−10717.
16. Aigner, S., Lingner, J., Goodrich, K. J., Grosshans, C. A., Shevchenko, A., Mann, M., and Cech, T. R. (2000) *EMBO J. 19*, 6230−6239.
17. McEachern, M. J., Krauskopf, A., and Blackburn, E. H. (2000) *Annu. Rev. Genet. 34*, 331−358.
18. Greider, C. W., and Blackburn, E. H. (1989) *Nature 337*, 331−337.
19. Lingner, J., Hughes, T. R., Shevchenko, A., Mann, M., Lundblad, V., and Cech, T. R. (1997) *Science 276*, 561−567.
20. Nakamura, T. M., Morin, G. B., Chapman, K. B., Weinrich, S. L., Andrews, W. H., Lingner, J., Harley, C. B., and Cech, T. R. (1997) *Science 277*, 955−959.
21. Chapon, C., Cech, T. R., and Zaug, A. J. (1997) *RNA 3*, 1337−1351.
22. Hinkley, C. S., Blasco, M. A., Funk, W. D., Feng, J., Villeponteau, B., Greider, C. W., and Herr, W. (1998) *Nucleic Acids Res. 26*, 532−536.
23. ten Dam, E., van Belkum, A., and Pleij, K. (1991) *Nucleic Acids Res. 19*, 6951.
24. Lingner, J., Hendrick, L. L., and Cech, T. R. (1994) *Genes Dev. 8*, 1984−1998.
25. McCormick-Graham, M., and Romero, D. P. (1995) *Nucleic Acids Res. 23*, 1091−1097.
26. Singer, M. S., and Gottschling, D. E. (1994) *Science 266*, 404−409.
27. McEachern, M. J., and Blackburn, E. H. (1995) *Nature 376*, 403−409.
28. Wolin, S. L., and Cedervall, T. (2002) *Annu. Rev. Biochem. 71*, 375−403.
29. Stefano, J. E. (1984) *Cell 36*, 145−154.
30. Mathews, M. B., and Francoeur, A. M. (1984) *Mol. Cell. Biol. 4*, 1134−1140.
31. Boelens, W. C., Palacios, I., and Mattaj, I. W. (1995) *RNA 1*, 273−283.
32. Pannone, B. K., Xue, D., and Wolin, S. L. (1998) *EMBO J. 17*, 7442−7453.
33. Shippen-Lentz, D., and Blackburn, E. H. (1990) *Science 247*, 546−552.
34. Yu, G.-L., Bradley, J. D., Attardi, L. D., and Blackburn, E. H. (1990) *Nature 344*, 126−132.
35. Sambrook, J., Fritsch, E. F., and Maniatis, T. (1989) *Molecular Cloning: a Laboratory Manual*, 2nd ed., Vol. 1, Cold Spring Harbor Laboratory Press, Plainview, NY.
36. O'Reilly, D. R., Miller, L. K., and Luckow, V. A. (1994) *Baculovirus Expression Vectors: a Laboratory Manual*, W. H. Freeman, New York.
37. Yoo, C. J., and Wolin, S. L. (1997) *Cell 89*, 393−402.
38. Roberson, A. E., Wolffe, A. P., Hauser, L. J., and Olins, D. E. (1989) *Nucleic Acids Res. 17*, 4699−4712.
39. Grimm, M., Brunen-Nieweler, C., Junker, V., Heckmann, K., and Beier, H. (1998) *Nucleic Acids Res. 26*, 4557−4565.
40. Postberg, J., Juranek, S. A., Feiler, S., Kortwig, H., Jonsson, F., and Lipps, H. J. (2001) *J. Cell Sci. 114*, 1861−1866.
41. Ammermann, D., Steinbruck, G., von Berger, L., and Hennig, W. (1974) *Chromosoma 45*, 401−429.
42. Wang, L., Dean, S. R., and Shippen, D. E. (2002) *Nucleic Acids Res. 30*, 4032−4039.
43. Hendrick, J. P., Wolin, S. L., Rinke, J., Lerner, M. R., and Steitz, J. A. (1981) *Mol. Cell. Biol. 1*, 1138−1149.
44. Yoo, C. J., and Wolin, S. L. (1994) *Mol. Cell. Biol. 14*, 5412−5424.
45. Ohndorf, U. M., Steegborn, C., Knijff, R., and Sondermann, P. (2001) *J. Biol. Chem. 276*, 27188−27196.
46. Ehresmann, C., Baudin, F., Mougel, M., Romby, P., Ebel, J. P., and Ehresmann, B. (1987) *Nucleic Acids Res. 15*, 9109−9128.
47. Bhattacharyya, A., and Blackburn, E. H. (1994) *EMBO J. 13*, 5721−5731.
48. Zaug, A. J., and Cech, T. R. (1995) *RNA 1*, 363−374.
49. Sperger, J. M., and Cech, T. R. (2001) *Biochemistry 40*, 7005−7016.
50. Antal, M., Boros, E., Solymosy, F., and Kiss, T. (2002) *Nucleic Acids Res. 30*, 912−920.
51. Prescott, D. M. (1994) *Microbiol. Rev. 58*, 233−267.
52. Olins, D. E., and Olins, A. L. (1994) *Int. Rev. Cytol. 153*, 137−170.
53. Fang, G., and Cech, T. R. (1995) *J. Cell Biol. 130*, 243−253.
54. Long, K. S., Cedervall, T., Walch-Solimena, C., Noe, D. A., Huddleston, M. J., Annan, R. S., and Wolin, S. L. (2001) *RNA 7*, 1589−1602.
55. Beattie, T. L., Zhou, W., Robinson, M. O., and Harrington, L. (1998) *Curr. Biol. 8*, 177−180.
56. Tesmer, V. M., Ford, L. P., Holt, S. E., Frank, B. C., Yi, X., Aisner, D. L., Ouellette, M., Shay, J. W., and Wright, W. E. (1999) *Mol. Cell. Biol. 19*, 6207−6216.
57. Ford, L. P., Shay, J. W., and Wright, W. E. (2001) *RNA 7*, 1068−1075.
58. Lewis, J. D., and Tollervey, D. (2000) *Science 288*, 1385−1389.
59. Gall, J. G. (2000) *Annu. Rev. Cell Dev. Biol. 16*, 273−300.
60. Narayanan, A., Lukowiak, A., Jady, B. E., Dragon, F., Kiss, T., Terns, R. M., and Terns, M. P. (1999) *EMBO J. 18*, 5120−5130.
61. Etheridge, K. T., Banik, S. S., Armbruster, B. N., Zhu, Y., Terns, R. M., Terns, M. P., and Counter, C. M. (2002) *J. Biol. Chem. 277*, 24764−24770.
62. Lukowiak, A. A., Narayanan, A., Li, Z. H., Terns, R. M., and Terns, M. P. (2001) *RNA 7*, 1833−1844.
63. Bachand, F., Boisvert, F. M., Cote, J., Richard, S., and Autexier, C. (2002) *Mol. Biol. Cell 13*, 3192−3202.
64. Wong, J. M., Kusdra, L., and Collins, K. (2002) *Nat. Cell Biol. 4*, 731−736.
65. Chang, Y. N., Kenan, D. J., Keene, J. D., Gatignol, A., and Jeang, K. T. (1994) *J. Virol. 68*, 7008−7020.
66. Goodier, J. L., Fan, H., and Maraia, R. J. (1997) *Mol. Cell. Biol. 17*, 5823−5832.
67. Maraia, R. J., and Intine, R. V. (2001) *Mol. Cell. Biol. 21*, 367−379.
68. Sobel, S. G., and Wolin, S. L. (1999) *Mol. Biol. Cell 10*, 3849−3862.
69. Simons, F. H., Rutjes, S. A., van Venrooij, W. J., and Pruijn, G. J. (1996) *RNA 2*, 264−273.
70. Grimm, C., Lund, E., and Dahlberg, J. E. (1997) *EMBO J. 16*, 793−806.
71. Collins, K., and Gandhi, L. (1998) *Proc. Natl. Acad. Sci. U.S.A. 95*, 8485−8490.

BI034121Y